JACS
JOURNAL OF THE AMERICAN CHEMICAL SOCIETY
pubs.acs.org/JACS
Article

Enantioselective C(sp^3)−H Functionalization of Oxacycles via Photo-HAT/Nickel Dual Catalysis

Sheng Xu, Yuanyuan Ping, Wei Li, Haoyun Guo, Yinyan Su, Ziyang Li, Minyan Wang,* and Wangqing Kong*

Cite This: https://doi.org/10.1021/jacs.2c12481
Read Online

ABSTRACT: The selective functionalization of ubiquitous but inert C−H bonds is highly appealing in synthetic chemistry, but the direct transformation of hydrocarbons lacking directing groups into high-value chiral molecules remains a formidable challenge. Herein, we develop an enantioselective C(sp^3)−H functionalization of undirected oxacycles via photo-HAT/nickel dual catalysis. This protocol provides a practical platform for the rapid construction of high-value and enantiomerically enriched oxacycles directly from simple and abundant hydrocarbon feedstocks. The synthetic utility of this strategy is further demonstrated in the late-stage functionalization of natural products and the synthesis of many pharmaceutically relevant molecules. Experimental and density functional theory calculation studies provide detailed insights into the mechanism and the origin of enantioselectivity for the asymmetric C(sp^3)−H functionalization.

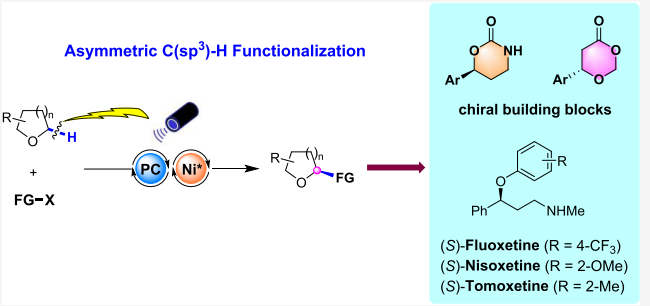

INTRODUCTION

The enantioselective functionalization of inert C(sp^3)−H bonds[1−4] is undoubtedly a transformative approach for the construction of high-value-added chiral molecules due to their atom and step economy as well as the abundance of starting materials (Scheme 1a). However, the regio- and enantioselective transformation of these hydrocarbons remains extremely challenging due to their inherent chemical inertness and slightly different reactivity of C(sp^3)−H bonds. Among the few available strategies, transition-metal-catalyzed directing group-assisted C−H activation has emerged as a key strategy for the direct and enantioselective functionalization of C(sp^3)−H bonds.[5,6] The concerted metal carbenoid/nitrenoid C−H insertion reaction also enables the direct enantioselective conversion of hydrocarbons to chiral molecules.[7,8] Despite these significant advances, there remains a strong demand for developing efficient methods for converting hydrocarbon feedstocks into valuable chiral molecules.

In recent years, the merger of the hydrogen atom transfer (HAT) process[9−11] with transition metal catalysis has shown considerable potential in the direct functionalization of C(sp^3)−H bonds.[12−16] In particular, photoredox and nickel dual catalysis, pioneered by MacMillan,[17] Molander,[18] and Doyle[17] et al., has emerged as a powerful tool for C(sp^3)−H functionalization.[19−29] Despite enormous efforts, the enantioselective transformation of hydrocarbons remains largely undeveloped and limited to α-amino[30−33] and benzylic[34−36] C−H bonds with relatively low bond dissociation energies. This quest is particularly arduous when it comes to the asymmetric C(sp^3)−H functionalization of undirected heterocycles, which are notoriously difficult to handle in enantioselective processes. Although the α-arylation of cyclic amides has been addressed, the benzoyl protecting group is indispensable not only to modulate the BDEs of the α-amino C−H bonds but also to act as a functional handle for stereoselective control.[30−33] Given that planar oxacycles have similar steric hindrance and lack of a functional handle, catalytic enantiofacial differentiation of small oxacycles is formidably challenging (Scheme 1b). Martin and co-workers developed an elegant strategy for asymmetric C−H arylation of THF through the synergy of triplet-excited ketones and nickel catalysts. Nevertheless, only moderate enantioselectivity (54% ee) was achieved (Scheme 1c).[37]

Inspired by the recent reports on Ni-photocatalyzed dehydrogenative[38−40] and Ni-catalyzed asymmetric Heck coupling reactions,[41−43] we reasoned that a dual photoredox/nickel-catalyzed dehydrogenation of saturated heterocycles followed by an asymmetric Heck coupling strategy might address the above-mentioned challenges (Scheme 1d).

Received: November 23, 2022

https://doi.org/10.1021/jacs.2c12481
J. Am. Chem. Soc. XXXX, XXX, XXX−XXX

Scheme 1. Asymmetric C(sp^3)−H Functionalization of Feedstock Hydrocarbons

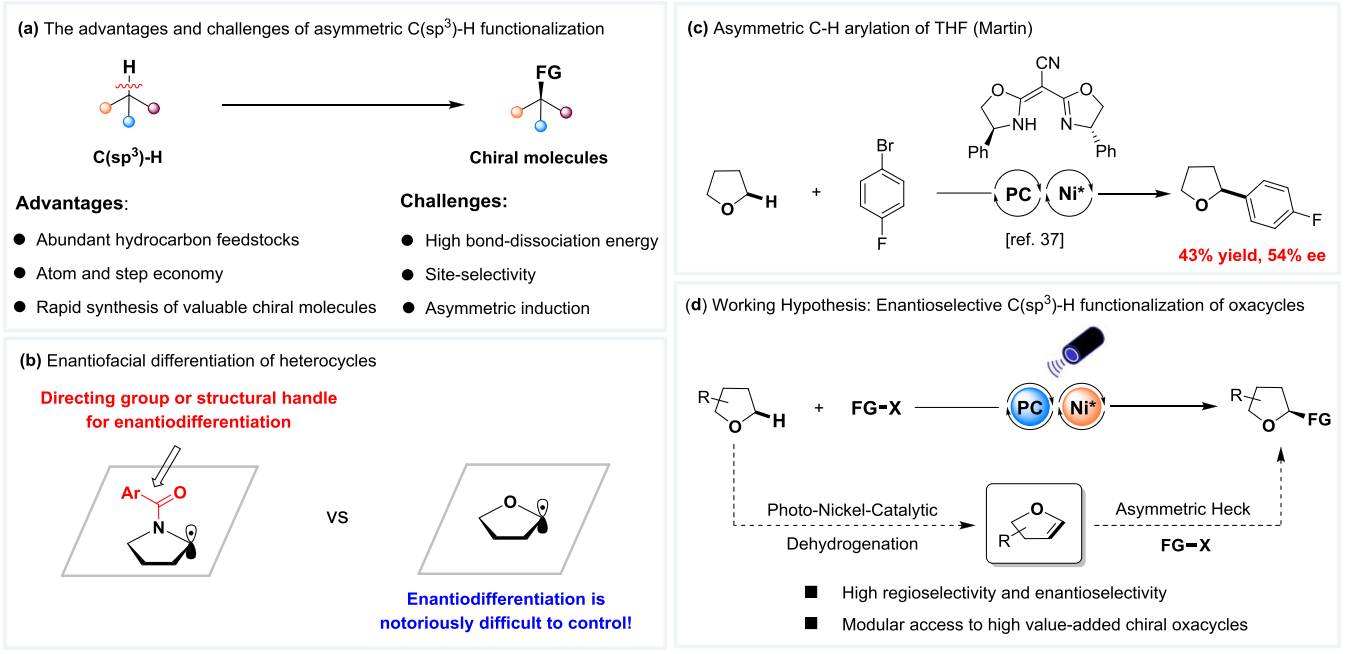

This article discloses our efforts to develop asymmetric C(sp^3)−H functionalization of undirected oxacycles by utilizing cooperative catalysts consisting of a tunable chiral PHOX−nickel catalyst and a commercially available diary ketone photocatalyst. The reaction proceeds under very mild conditions and features broad substrate scope, covering a variety of oxacycles and diverse (hetero)aryl and alkenyl bromides, with good functional group compatibility and excellent enantioselectivity. Notably, this method provides a single-step conversion of abundantly available hydrocarbons to chiral α-functionalized oxacycles, which are often found as key structural elements in biologically active molecules or serve as chiral building blocks in drug synthesis.

RESULTS AND DISCUSSION

We started our investigations by studying the asymmetric C(sp^3)−H arylation of tetrahydrofuran **1** with ethyl 4-bromobenzoate **2** (Table 1). Extensive evaluation of the reaction parameters identified that the combination of $NiCl_2$·DME, the chiral PHOX ligand **L1**, Na_2CO_3, and the diaryl ketone **PC1** as a photo-HAT catalyst[37,44−46] under irradiation with 10 W light-emitting diodes (LEDs) at −5 °C provided the desired product **3** in 75% yield and 90% e.e. (entry 1, condition A). Attempts to use other widely used photo-HAT catalysts $Ir[dF(CF_3)ppy]_2(dtbbpy)PF_6$[47−52] or TBADT[53] failed to obtain the desired product (entries 2 and 3). The electronic effects on the diaryl ketones have a non-negligible impact on the reaction efficiency (entries 4 and 5). Screening of several chiral ligand scaffolds revealed that previously commonly used bis(oxazoline), pyridyloxazoline, and bis(imidazoline) ligands (**L4**−**L6**) were ineffective (entries 6−10). As shown in entries 11 and 12, other chlorine-free nickel sources such as $Ni(COD)_2$ or $NiBr_2$·DME could also be used as a precatalyst, thus indicating that this approach is different from previously reported chlorine radical-mediated HAT processes (entries 11 and 12).[33,49,54−57] This asymmetric C(sp^3)−H functionalization could also be performed in ethyl acetate as a solvent, using 20 equiv of the C−H precursor, providing a complementary protocol for other oxacycles (entry 13, condition B). When the reaction was carried out at room temperature, the ee value decreased slightly (entry 14). Control experiments revealed that all parameters, including nickel catalyst, light, photocatalyst, and Na_2CO_3, were essential for this transformation (entries 15−18).

With the optimal conditions in hand, we sought to examine the generality of the asymmetric C(sp^3)−H functionalization protocol. As shown in Scheme 2, aryl bromides with various functional groups such as ester (**3** and **4**), ketone (**5**), aldehyde (**6**), nitrile (**7**), sulfone (**8**), trifluoromethyl (**9**), and fluorine (**10**) were perfectly tolerated. Notably, aryl chlorides (**11**−**13**), which are susceptible to Ni-catalyzed cross-couplings, were found to be accommodated, thereby opening additional avenues for derivatization of the resulting products. In addition, electron-neutral aryl bromides were also reactive substrates (**14** and **15**). To demonstrate the robustness of this protocol, heteroaryl bromides were also investigated. Pyridine, quinoline, and dibenzothiophene could be successfully incorporated into the target products (**16** to **19**). Furthermore, aryl bromides are derived from chiral pools or complex biologically important molecules, such as D-phenylalaninate (**20**), L-menthol (**21**), D-allofuranose (**22**), sertraline (**23**), sulbactam (**24**), cholesterol (**25**), and estrone (**26**), did not have any detrimental effect on efficiency (62−78%) and diastereoselective (>95/5, d.r.), showcasing the potential of this transformation for late-stage functionalization of complex molecules.

The asymmetric photochemical C(sp^3)−H functionalization was not limited to aryl bromides, as alkenyl bromides were also effective coupling partners. Activated alkenyl bromides, such as 2-bromo-1*H*-indene and 3-bromocyclohex-2-en-1-one, and inactivated alkenyl bromide, such as azacycloalkenyl bromide, were coupled with tetrahydrofuran to provide the corresponding optically active products **27**−**29** in good yields with excellent enantioselectivities.

Although the asymmetric C(sp^3)−H alkylation of tetrahydrofuran fails, formally, asymmetric C(sp^3)−C(sp^3) cross-

https://doi.org/10.1021/jacs.2c12481
J. Am. Chem. Soc. XXXX, XXX, XXX−XXX

Table 1. Optimization of the Reaction Conditions[a,b]

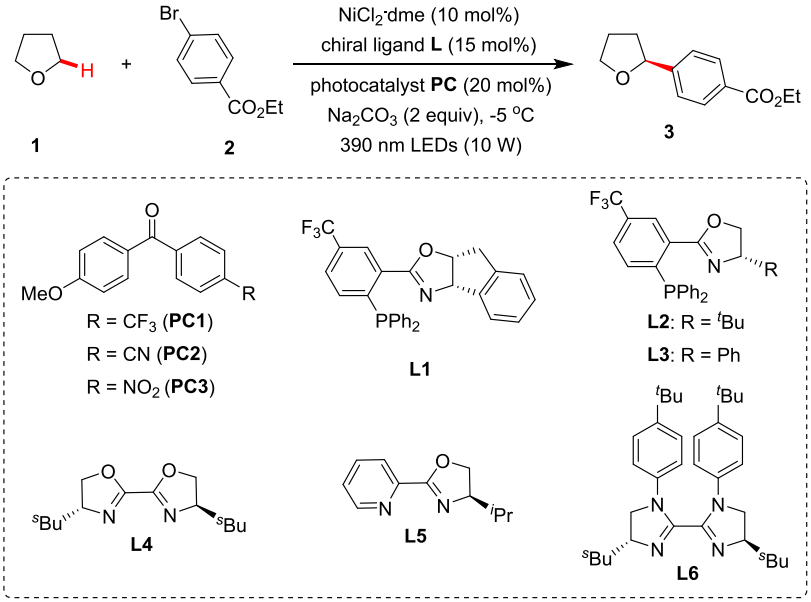

entry	photocatalyst	ligand	yield of 3 (%)[b]	ee of 3 (%)[c]
1	**PC1**	**L1**	75	90
2	$Ir[dF(CF_3)ppy]_2$ (dtbbpy)PF_6	**L1**	trace	
3	TBADT	**L1**	trace	
4	**PC2**	**L1**	28	88
5	**PC3**	**L1**	trace	
6	**PC1**	**L2**	20	85
7	**PC1**	**L3**	56	72
8	**PC1**	**L4**	8	39
9	**PC1**	**L5**	16	7
10	**PC1**	**L6**	54	55
11[d]	**PC1**	**L1**	65	80
12[e]	**PC1**	**L1**	34	31
13[f]	**PC1**	**L1**	68	90
14[g]	**PC1**	**L1**	66	87
15[h]	**PC1**	**L1**	n.d.	
16	**none**	**L1**	n.d.	
17[i]	**PC1**	**L1**	n.d.	
18[j]	**PC1**	**L1**	n.d.	

[a]Reaction conditions: **2** (0.2 mmol, 1 equiv), $NiCl_2$·DME (10 mol %), ligand (15 mol %), Na_2CO_3 (2 equiv), photocatalyst (20 mol %), and tetrahydrofuran **1** (2 mL, 0.1 M) under the irradiation of LEDs (10 W, 390 nm) at −5 °C for 72 h. [b]Isolated yields. [c]The ee values were determined by HPLC using a chiral stationary phase. [d]$Ni(COD)_2$ (10 mol %) was used instead of $NiCl_2$·DME. [e]$NiBr_2$·DME (10 mol %) was used instead of $NiCl_2$·DME. [f]Reaction performed with tetrahydrofuran (20 equiv) in EtOAc (2 mL, 0.1 M). [g]Reaction performed at room temperature. [h]Without nickel catalyst. [i]Reaction performed in the dark. [j]Reaction performed in the absence of Na_2CO_3. TBADT: tetrabutylammonium decatungstate.

couplings could be achieved via a one-pot C(sp^3)−H alkenylation and palladium−carbon reduction sequence. As shown, the product **30** bearing two stereocenters was obtained in 71% yield with high diastereoselectivity (15:1 d.r.). This protocol offers a complementary strategy to address the notorious problems of enantioselectivity and diastereoselectivity control in C(sp^3)−C(sp^3) cross-coupling reactions.

We next turned our attention to examine the scope of oxacycles. As depicted in Scheme 3, a wide range of oxacycles underwent asymmetric C(sp^3)−H arylation smoothly, delivering the corresponding products in high efficiency with excellent stereoselectivity. Arylation of tetrahydrofuran-D_8 successfully afforded the deuterium-labeled product **32** in 81% yield and 94% ee. 2-Methyl tetrahydrofuran **33** was selectively arylated on the less sterically hindered C(sp^3)−H bond. Methyl (*S*)-tetrahydrofuran-2-carboxylate **35** was readily arylated to deliver the desired product **36** in 70% yield and greater than 25:1 diastereoselectivity. These results clearly show that the observed high enantioselectivity depends on the structure of the ligand rather than the substrate. The absolute configuration of the product **36** was determined by single-crystal X-ray diffraction analysis of its hydrolysis product **37**. Furthermore, tetrahydrofuran-3-one **38**, a reactive substrate, produced the desired product **39** in 64% yield and 92% ee. γ-Butyrolactone **40** was a competent substrate that could be coupled with aryl bromide to provide 4-aryl γ-butyrolactone **41**, which can be used to synthesize many biologically active compounds, such as cryptophycin and tetrahydrolipstatin. In substrates **38** and **40**, the more labile electrophilic α-hydrogen was not activated by the electrophilically excited ketone

https://doi.org/10.1021/jacs.2c12481
J. Am. Chem. Soc. XXXX, XXX, XXX−XXX

Scheme 2. Scope of Aryl and Alkenyl Bromide Coupling Partners

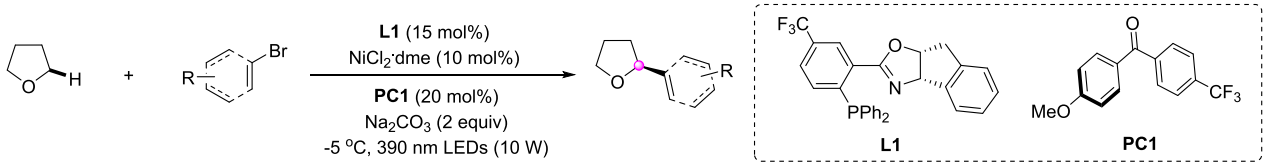

Aryl Bromides

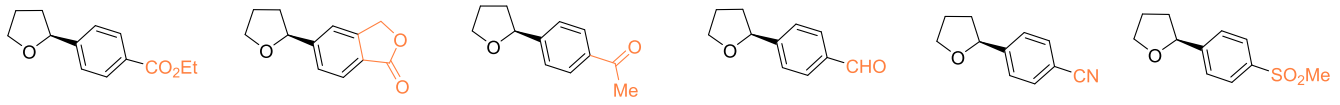

3, 75%, 90% ee | **4**, 60%, 93% ee | **5**, 92%, 92% ee | **6**, 67%, 90% ee | **7**, 83%, 92% ee | **8**, 72%, 92% ee

9, 69%, 90% ee | **10**, 67%, 88% ee | **11**, 64%, 90% ee | **12**, 67%, 89% ee | **13**, 69%, 88% ee | **14**, 65%, 91% ee

Heteroaryl Bromides

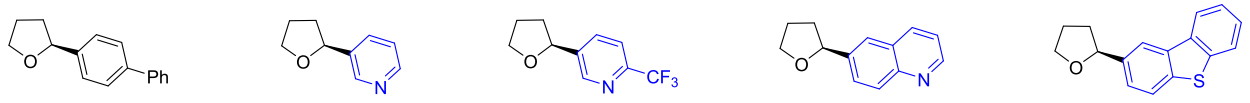

15, 61%, 88% ee | **16**, 63%, 91% ee | **17**, 76%, 91% ee | **18**, 75%, 92% ee | **19**, 66%, 88% ee

Aryl Bromides Derived from Complex Molecules

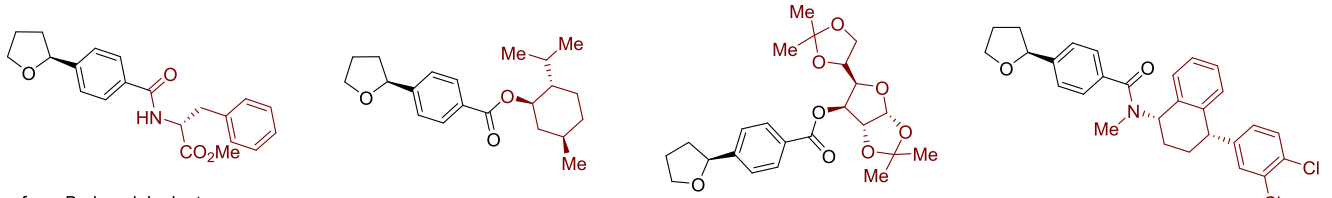

from *D*-phenylalaninate
20, 66%, > 95:5 d.r.

from *L*-menthol
21, 62%, > 95:5 d.r.

from *D*-allofuranose
22, 78%, > 95:5 d.r.

from Sertraline
23, 72%, > 95:5 d.r.

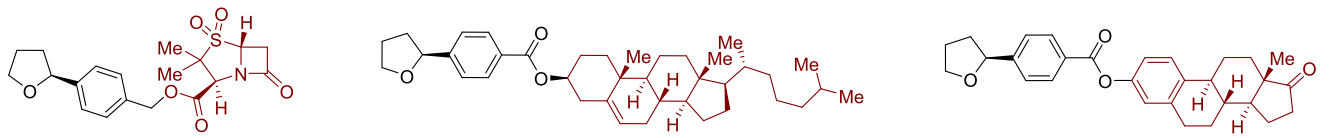

from Sulbactam
24, 62%, > 95:5 d.r.

from Cholesterol
25, 68%, > 95:5 d.r.

from Estrone
26, 64%, > 95:5 d.r.

Alkenyl Bromides

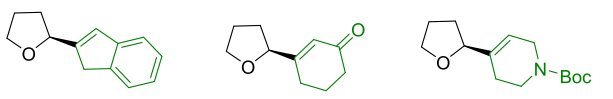

27, 70%, 91% ee | **28**, 60%, 90% ee | **29**, 71%, 88% ee

Formal Asymmetric C(sp^3)-C(sp^3) Cross-Coupling

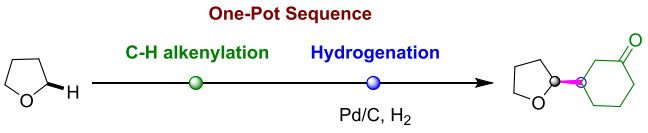

30, 71%, > 15:1 d.r.

abstractor due to the partial negative charge on the initial C-centered radical, making the corresponding transition state unfavorable. Cyclic ethers of various ring sizes, such as oxetane **42** and oxane **44**, were well tolerated (**43** and **45**). 2,5-Dihydrofuran **46** and 2,3-dihydrofuran **47** proceeded smoothly, but the double bond in the resulting product was reduced. This may be due to the formation of stable aromatic furans and Ni−H species by elimination of β-hydrogen, which can further undergo migratory insertion with **46** and **47**. Multisubstituted cyclic ether **48** was tolerated, furnishing the desired product **49** in 63% yield with excellent diastereoselectivity (>95/5 d.r.).

Remarkably, we found that the electronegativity of the protecting groups on the oxygen atom can tune the dissociation energy of the C(sp^3)−H bond, enabling regiodivergent and enantioselective C(sp^3)−H functionaliza-

https://doi.org/10.1021/jacs.2c12481
J. Am. Chem. Soc. XXXX, XXX, XXX−XXX

Scheme 3. Scope of Undirected Oxacycles[a,b,c]

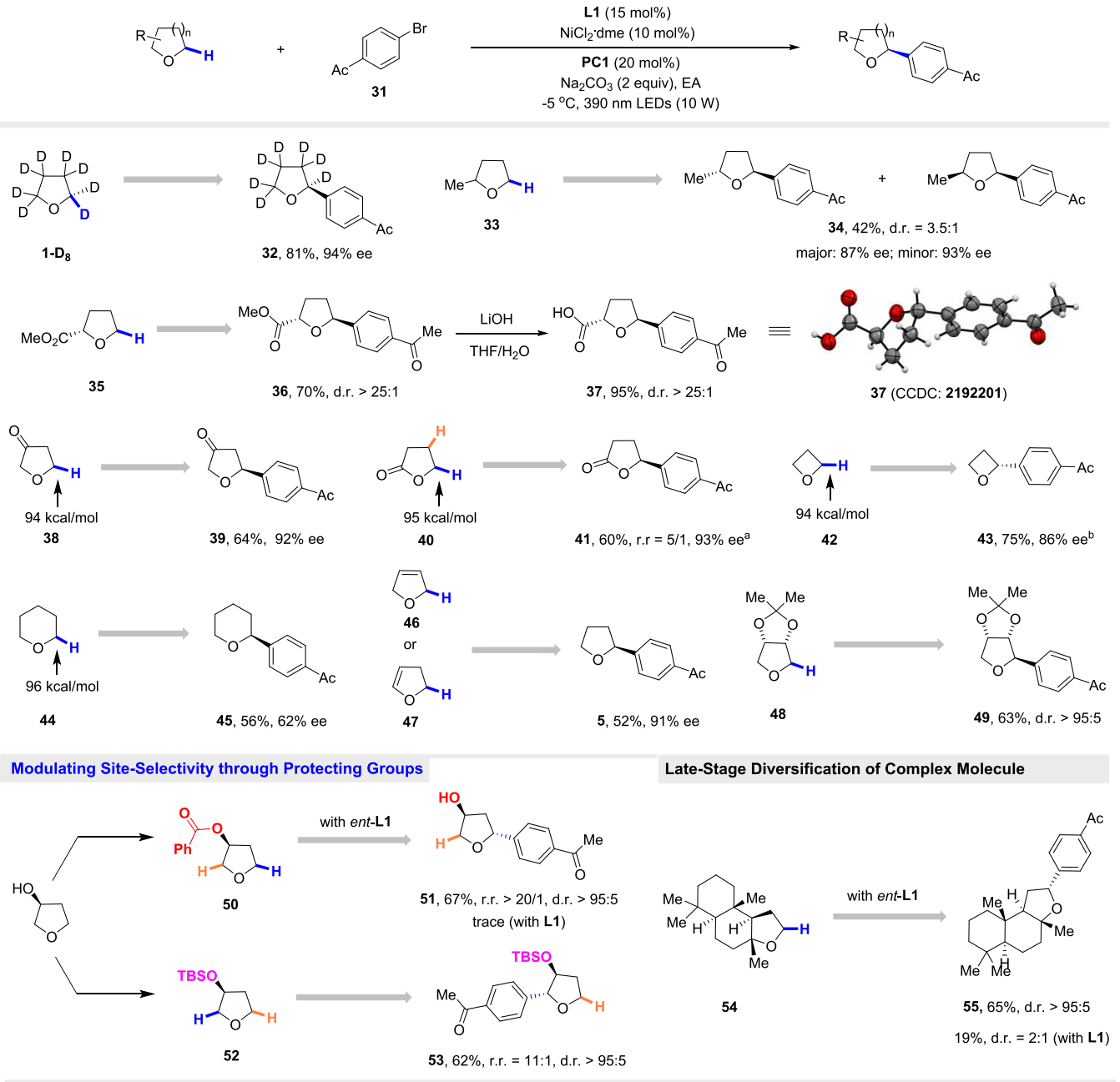

[a]Reaction conditions: 31 (0.2 mmol, 1 equiv), $NiCl_2$·DME (10 mol %), ligand (15 mol %), Na_2CO_3 (2 equiv), photocatalyst (20 mol %), and oxacycle substrate (20 equiv) in ethyl ecatate (2 mL, 0.1 M) under the irradiation of LEDs (10 W, 390 nm) at −5 °C for 72 h. [b]This reaction was conducted at 25 °C using **PC2** (20 mol %) as photosensitizers in γ-butyrolactone (2 mL). [c]**L2** was used. *ent*-**L1** is the enantiomer of **L1**.

tion. As shown in Scheme 3, the benzoyl-protected (*S*)-tetrahydrofuran-3-ol **50** underwent selective C(sp^3)−H arylation at the 5-position to afford **51** in 67% yield with greater than 20:1 diastereoselectivity. In contrast, TBS-protected (*S*)-tetrahydrofuran-3-ol **52** was selectively arylated at the 2-position to furnish **53** in 62% yield with greater than 11:1 diastereoselectivity. Our protocol is also feasible for the late-stage functionalization of complex molecules. Direct arylation of (−)-ambroxide **54** delivered **55** in 65% yield with excellent diastereoselectivity with *ent*-**L1** (>95:5 d.r.). The use of ligand **L1** resulted in low yield and diastereoselectivity, suggesting that chiral ligands are the key to regulating the stereoselectivity of the reaction.

The utility of this asymmetric C(sp^3)−H functionalization reaction was demonstrated by scale-up reaction and applications in the synthesis of chiral building blocks and biologically active natural products and drugs. The scaled-up reaction using 1.0 g of 4′-bromoacetophenone **31** and tetrahydrofuran provided 0.64 g of product **5** with no change in enantioselectivity (Scheme 4i). Aryl pinacol boronate was perfectly accommodated and provided the corresponding product **56** in 62% yield and 91% ee, which could be converted into adenosine monophosphate-activated protein kinase (AMPK) activator for prevention and treatment of AMPK-mediated disorders (Scheme 4ii).[58] Chiral γ-butyrolactone **57** was converted to cyclic carbamate **58** by

https://doi.org/10.1021/jacs.2c12481
J. Am. Chem. Soc. XXXX, XXX, XXX−XXX

Scheme 4. Scale-Up Synthesis and Applications in the Synthesis of Biologically Active Molecules and Drugs[a]

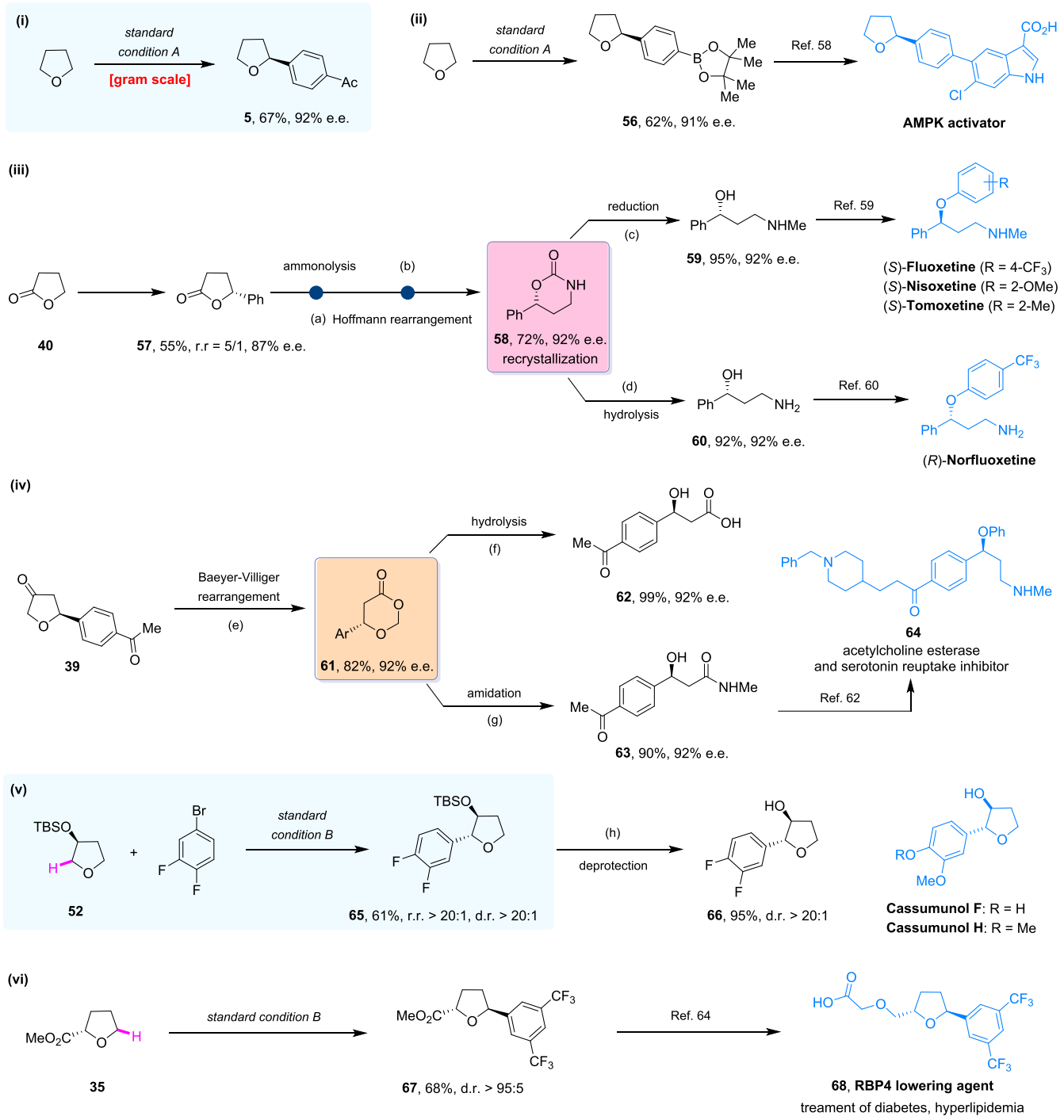

[a]Reaction Conditions: (a) $NH_3{\cdot}H_2O$, MeOH, rt; (b) $PhI(OAc)_2$ (2.0 equiv), MeCN, 40 °C; (c) $LiAlH_4$ (3.0 equiv), THF, reflux; (d) KOH (2.0 equiv), ^{i}PrOH, H_2O, reflux; (e) ^{m}CPBA (2.0 equiv), $NaHCO_3$ (1.0 equiv), DCM, rt; (f) HCl (1N), MTBE, rt; (g) MeNH2. HCl (2.0 equiv), KOAc (2.0 equiv), THF, rt; (h) TBAF, THF, rt; (i) potassium phthalimide (1.2 equiv), KI (0.1 equiv), DMF, 70 °C; (j) NH_2NH_2. H_2O, EtOH, 80 °C; (k) HCl (1 M), THF, rt; (l) NH_3. BH_3 (1.1 equiv), NaHMDS (1.5 equiv), THF, rt; (m) TBAF, THF, rt; HCl (1 M), THF, rt. ^{m}CPBA = 3-chloroperoxybenzoic acid.

ammonolysis and subsequent Hoffmann rearrangement. Reduction of carbamate **58** with $LiAlH_4$ afforded 1,3-aminoalcohol **59**, a common intermediate for the chemical synthesis of the important antidepressants (*S*)-tomoxetine, (*S*)-nisoxetine, and (*S*)-fluoxetine.[59] Carbamate **58** was hydrolyzed to 1,3-aminoalcohol **60**, which could be further converted to (*R*)-norfluoxetine, a potent and selective inhibitor of neural serotonin reuptake (Scheme 4iii).[60] In addition, the enantioenriched dioxanone **61** is a valuable and versatile synthetic building block that could be readily obtained in 82% yield by Baeyer−Villiger oxidation of **39** with *m*-CPBA while maintaining enantioselectivity.[61] Hydrolysis and aminolysis of

https://doi.org/10.1021/jacs.2c12481
J. Am. Chem. Soc. XXXX, XXX, XXX−XXX

Scheme 5. Mechanistic Investigation

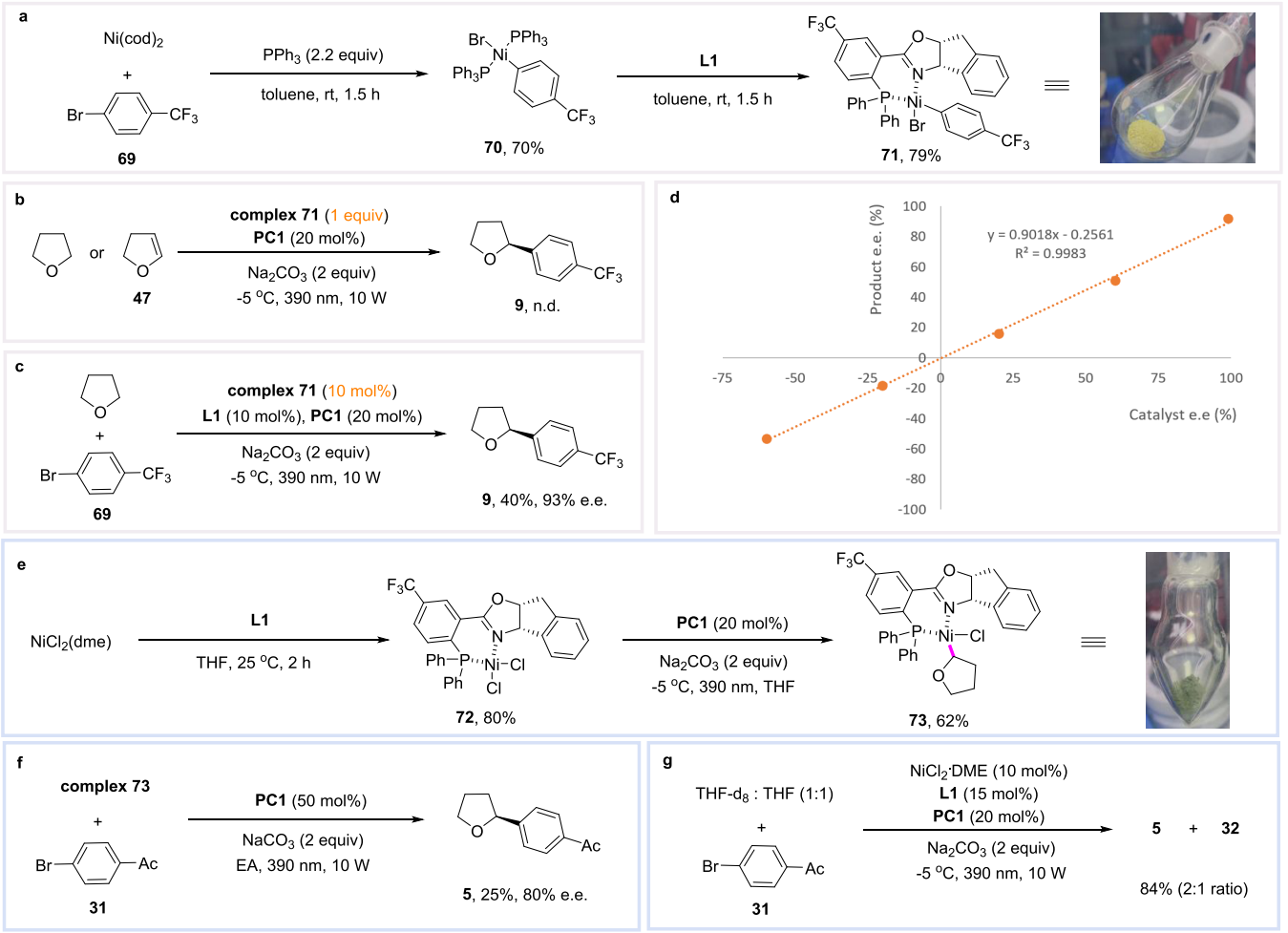

dioxanone **61** gave the corresponding *β*-hydroxycarboxylic acid **62** and *β*-hydroxy amide **63**, respectively (Scheme 4iv). Amide **63** is an intermediate in the synthesis of compound **64**, which exhibits inhibitory activity against acetylcholine esterase and selective serotonin reuptake.[62] Trans-*ortho*-arylation of TBS-protected **52** afforded **65** in 61% yield with high regioselectivity (>20:1, r.r.) and diastereoselectivity (>20:1, d.r.). Removal of the TBS protecting group gave product **66**, an analog of the natural products cassumunols **F** and **H** (Scheme 4v).[63] Moreover, retinol binding protein 4 (RBP4) lowering agent **68** for the treatment of diabetes and hyperlipidemia could be synthesized from the asymmetric C(sp^3)−H arylation product **67** (Scheme 4vi).[64]

To gain some insight into the reaction mechanism, a variety of mechanistic experiments were designed (Scheme 5). Chiral Ar−Ni(II) complex **71** was prepared by ligand exchange of complex **70** with **L1** (Scheme 5a). The stoichiometric reaction of complex **71** with THF or 2,3-dihydrofuran **47** failed to afford the desired product **9** (Scheme 5b). If the nickel complex **71** was used in catalytic amount, product **9** was obtained in 40% yield with 93% ee (Scheme 5c). These results indicated that the Ar−Ni(II) complex might not be the active intermediate for this reaction. Moreover, a linear effect between the enantiomeric excess of product **5** and the enantiopurity of ligand **L1** was examined, indicating that a 1:1 ratio of nickel to ligand was involved in the enantio-determining step (Scheme 5d). Exposure of THF and **L1**-coordinated nickel dichloride **72** to light generated alkyl−nickel complex **73** (Scheme 5e). Notably, the cross-coupling reaction of complex **73** with aryl bromide **31** provided the expected product **5** in 25% yield. This result provides solid evidence that the triplet alkyl−nickel complex **73** is a key intermediate for this transformation (Scheme 5f). Furthermore, the measured kinetic isotope effect (KIE) value (2.0) suggests that the HAT process might be involved in the rate-determining step (Scheme 5g).

To investigate the origin of enantioselectivity, density functional theory (DFT) calculations were also performed on the model reaction of tetrahydrofuran and 4-bromoacetophenone **31** at the *ω*b97xd/6-311+G(d,p)-SDD(Ni)/SMD-(THF)/B3LYP-D3/6-31G(d)-LANL2DZ(f)(Ni) level of theory. The calculated results involving photocatalytic and Ni-catalytic cycles are shown in Scheme 6.[65] Initially, upon irradiation with 10 W purple light-emitting diodes (LEDs), the ketone sensitizer **PC1** is excited to generate the triplet-excited state **INT1A**, which is set as the relative zero point in the photocatalytic cycle (Scheme 6a). The excited **INT1A** can reduce the excited single ^{S}**Ni^{II}** complex to ^{D}**Ni^{I}** with an exothermic energy of 11.2 kcal·mol^{-1}. Subsequently, the generated **INT2A** captures the hydrogen atom in tetrahydrofuran through the transition state **TS1A** with an activation energy of 4.6 kcal·mol^{-1} to produce a carbon-centered radical **A** that can engage in nickel-catalyzed cross-coupling reactions. Further deprotonation regenerates a ketone sensitizer **PC1** to

https://doi.org/10.1021/jacs.2c12481
J. Am. Chem. Soc. XXXX, XXX, XXX−XXX

Scheme 6. DFT Investigation

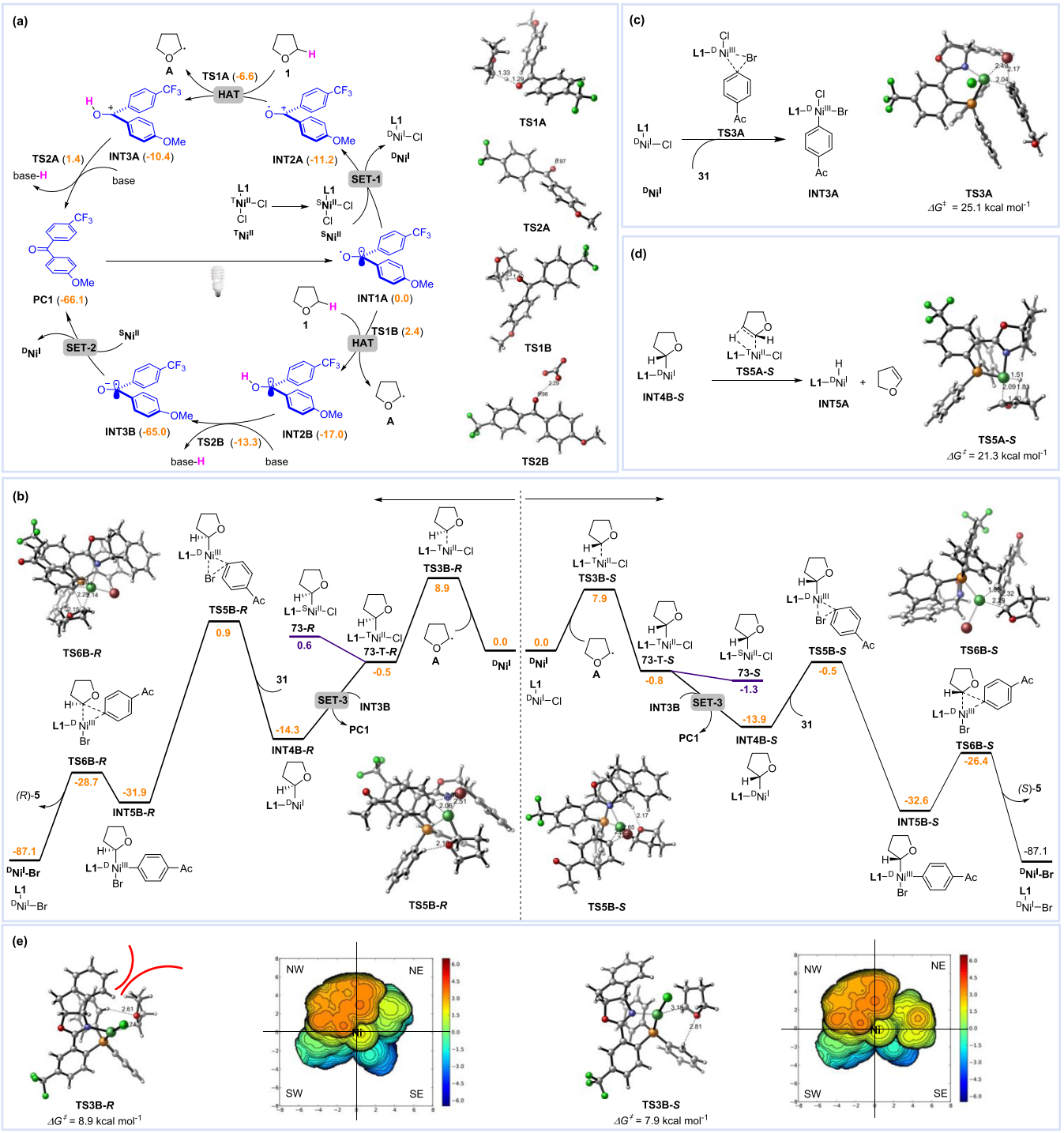

complete the photocatalytic cycle. Alternatively, **INT1A** could also be reductively quenched by feedstock hydrocarbons via the HAT process to generate radical **A** and acidic alcohol radical **INT2B** (Figure S2, green line). In the presence of carbonate anions, **INT2B** is deprotonated through the transition state **TS2B** with an energy barrier of 3.7 kcal·mol^{-1} to afford the intermediate **INT3B**, which then reduces ^{S}**Ni^{II}** to ^{D}**Ni^{I}** via a single-electron transfer (SET) process with a tremendous exothermic energy. Given the abundance of THF, we speculate that a photocatalytic cycle involving HAT, deprotonation, and subsequent SET processes is the main pathway. This process generates the Ni(I) species ^{D}**Ni^{I}** and the carbon-centered radical **A** for the subsequent Ni-catalytic cycle.

In the nickel catalytic cycle (Scheme 6b), DFT computation starts from the key Ni(I) intermediate ^{D}**Ni^{I}**. In contrast to the oxidative addition of **31** through the transition state **TS3A**, the resulting ^{D}**Ni^{I}** is prior to undergo radical addition to radical **A** via transition states **TS3B-*S*** or **TS3B-*R*** (7.9 kcal·mol^{-1} for **TS3B-*S*** and 8.9 kcal mol^{-1} for **TS3B-*R*** vs 25.1 kcal·mol^{-1} for **TS3A**, Scheme 6c).[66] The radical addition step is an enantio-determining step, and the relative Gibbs free energy of the transition state **TS3B-*S*** is 1.0 kcal mol^{-1} lower than that of

https://doi.org/10.1021/jacs.2c12481
J. Am. Chem. Soc. XXXX, XXX, XXX−XXX

TS3B-*R*. The origin of enantioselectivity can be further visualized by steric maps around nickel using SambVca 2.1 tool (Scheme 6e).[67] The geometries of both transition states are tetrahedrons, where the orientation of the P atom is defined as *Z* axis and chiral ligand **L1** occupied both NW and SW quadrants of the steric map, extending into the NE and SE quadrants. Thus, a chiral pocket is created to accommodate radical **A**. In **TS3B-*S***, the distances between the O atom of radical **A** and the *ortho*-C−H bond of the P atom on the phenyl ring are 2.61 and 2.81 Å, respectively, indicating the existence of weak hydrogen bonds. For the disfavored transition state **TS3B-*R***, the CH_2 group adjacent to oxygen in radical **A** is proximal to the indene ring of chiral ligand **L1**, and such repulsion interaction increases the energy barrier of **TS3B-*R*** to 8.9 kcal·mol^{-1}, which is 1.0 kcal·mol^{-1} higher than the corresponding favored transition state **TS3B-*S*** (8.9 vs 7.9 kcal·mol^{-1}). The complex **73-*S*** is the resting state of the catalyst, which could be isolated and then converted into the triplet-state **73-T-*S*** with a slight energy barrier to participate in the catalytic cycle. The computational result is consistent with the control experiments shown in Scheme 5e and Scheme 5f. The SET processes between intermediates **73-T-*S*** and **INT3B** are thermodynamically favorable, affording the intermediate **INT4B-*S***.[68,69] The extensive computational analysis on the alkyl−Ni(I) species **INT4B-*S*** was also carried out (Scheme 6d). *β*-H elimination occurs via transition states **TS5A-*S*** with an activation energy of 21.3 kcal·mol^{-1}, giving byproducts 2,3-dihydrofuran and Ni(II)−H species **INT5A**. As a competing pathway, the oxidative addition of the intermediate **INT4B-*S*** with **31** has a lower activation free energy (14.4 *vs* 21.3 kcal mol^{-1}). The energy of the transition state **TS5B-*S*** is 14.4 kcal·mol^{-1}, which is located as the highest energy barrier in the overall reaction pathway and might be the rate-determining step. Subsequent reductive elimination via the transition state **TS6B-*S*** yields the desired *S*-configuration product (*S*)-**5** and regenerates the Ni(I) species ^{D}**Ni^{I}-Br** for the next catalytic cycle.

The reaction mechanism involving the Ni(I)−Ni(II) and Ni(I)−Ni(II)−Ni(IV) pathways has been well ruled out owing to the high energies required (see the Supporting Information for details).[70,71]

CONCLUSIONS

We report the development of an enantioselective C(sp^3)−H functionalization of oxacycles without exogenous directing groups by integrating photo-HAT and nickel catalysis. This protocol provides rapid and economic access to a wide range of high-value and enantiomerically enriched oxacycles directly from simple and abundant hydrocarbon feedstocks. The synthetic utility of this strategy is further demonstrated in the late-stage functionalization of natural products and the synthesis of many pharmaceutically relevant molecules. Experimental and density functional theory calculation studies provide detailed insights into the mechanism and the origin of enantioselectivity for the asymmetric C(sp^3)−H functionalization.

ASSOCIATED CONTENT

Supporting Information

The Supporting Information is available free of charge at https://pubs.acs.org/doi/10.1021/jacs.2c12481.

Experimental procedures and spectral data for all new products (PDF)

Accession Codes

CCDC 2192201 contains the supplementary crystallographic data for this paper. These data can be obtained free of charge via www.ccdc.cam.ac.uk/data_request/cif, or by emailing data_request@ccdc.cam.ac.uk, or by contacting The Cambridge Crystallographic Data Centre, 12 Union Road, Cambridge CB2 1EZ, UK; fax: +44 1223 336033.

AUTHOR INFORMATION

Corresponding Authors

Minyan Wang − *State Key Laboratory of Coordination Chemistry, School of Chemistry and Chemical Engineering, Nanjing University, Nanjing 210023, China*; Email: wangmy@nju.edu.cn

Wangqing Kong − *The Institute for Advanced Studies and Hongyi Honor College, Wuhan University, Wuhan 430072, China*; orcid.org/0000-0003-3260-0097; Email: wqkong@whu.edu.cn

Authors

Sheng Xu − *The Institute for Advanced Studies and Hongyi Honor College, Wuhan University, Wuhan 430072, China*

Yuanyuan Ping − *The Institute for Advanced Studies and Hongyi Honor College, Wuhan University, Wuhan 430072, China*

Wei Li − *The Institute for Advanced Studies and Hongyi Honor College, Wuhan University, Wuhan 430072, China*

Haoyun Guo − *The Institute for Advanced Studies and Hongyi Honor College, Wuhan University, Wuhan 430072, China*

Yinyan Su − *The Institute for Advanced Studies and Hongyi Honor College, Wuhan University, Wuhan 430072, China*

Ziyang Li − *The Institute for Advanced Studies and Hongyi Honor College, Wuhan University, Wuhan 430072, China*

Complete contact information is available at: https://pubs.acs.org/10.1021/jacs.2c12481

Notes

The authors declare no competing financial interest.

ACKNOWLEDGMENTS

Financial support was provided by the National Natural Science Foundation of China (grant no. 22171215 and 22171134), the Hubei Provincial Outstanding Youth Fund (2022CFA092), and the National Key R&D Program of China (2022YFA1503200). Y.P. thanks the China Postdoctoral Science Foundation (grant no. 2020M680108 and 2022T150495) and the Guangdong Basic and Applied Basic Research Foundation (grant no. 2022A1515110113). The authors also thank the High-Performance Computing Center of Nanjing University for doing the numerical calculations in this paper on its blade cluster system.

REFERENCES

(1) Zheng, C.; You, S.-L. Recent development of direct asymmetric functionalization of inert C-H bonds. *RSC Adv.* **2014**, *4*, 6173−6214.

(2) He, J.; Wasa, M.; Chan, K. S. L.; Shao, Q.; Yu, J.-Q. Palladium-Catalyzed Transformations of Alkyl C-H Bonds. *Chem. Rev.* **2017**, *117*, 8754−8786.

(3) Newton, C. G.; Wang, S.-G.; Oliveira, C. C.; Cramer, N. Catalytic enantioselective transformations involving C-H bond

cleavage by transition metal complexes. *Chem. Rev.* **2017**, *117*, 8908−8976.
(4) Zhang, C.; Li, Z.; Gu, Q.; Liu, X.-Y. Catalytic enantioselective C(sp^3)-H functionalization involving radical intermediates. *Nat. Commun.* **2021**, *12*, No. 475.
(5) Rouquet, G.; Chatani, N. Catalytic Functionalization of C(sp^2)-H and C(sp^3)-H Bonds by Using Bidentate Directing Groups. *Angew. Chem., Int. Ed.* **2013**, *52*, 11726−11743.
(6) Saint-Denis, T. G.; Zhu, R.-Y.; Chen, G.; Wu, Q.-F.; Yu, J.-Q. Enantioselective C(sp^3)-H bond activation by chiral transition metal catalysts. *Science* **2018**, *359*, No. eaao4798.
(7) Davies, H. M. L.; Liao, K. Dirhodium tetracarboxylates as catalysts for selective intermolecular C-H functionalization. *Nat. Rev. Chem.* **2019**, *3*, 347−360.
(8) Hayashi, H.; Uchida, T. Nitrene transfer reactions for asymmetric C-H amination: recent development. *Eur. J. Org. Chem.* **2020**, *2020*, 909−916.
(9) Cao, H.; Tang, X.; Tang, H.; Yuan, Y.; Wu, J. Photoinduced intermolecular hydrogen atom transfer reactions in organic synthesis. *Chem Catal.* **2021**, *1*, 523−598.
(10) Capaldo, L.; Ravelli, D.; Fagnoni, M. Direct Photocatalyzed Hydrogen Atom Transfer (HAT) for Aliphatic C-H Bonds Elaboration. *Chem. Rev.* **2022**, *122*, 1875−1924.
(11) Zhang, Z.; Chen, P.; Liu, G. Copper-catalyzed radical relay in C(sp^3)-H functionalization. *Chem. Soc. Rev.* **2022**, *51*, 1640−1658.
(12) Zhang, W.; Wang, F.; McCann, S. D.; Wang, D.; Chen, P.; Stahl, S. S.; Liu, G. Enantioselective cyanation of benzylic C-H bonds via copper-catalyzed radical relay. *Science* **2016**, *353*, 1014−1018.
(13) Murphy, J. J.; Bastida, D.; Paria, S.; Fagnoni, M.; Melchiorre, P. Asymmetric catalytic formation of quaternary carbons by iminium ion trapping of radicals. *Nature* **2016**, *532*, 218−222.
(14) Mazzarella, D.; Crisenza, G. E. M.; Melchiorre, P. Asymmetric Photocatalytic C-H Functionalization of Toluene and Derivatives. *J. Am. Chem. Soc.* **2018**, *140*, 8439−8443.
(15) Li, Y.; Lei, M.; Gong, L. Photocatalytic regio- and stereoselective C(sp^3)−H functionalization of benzylic and allylic hydrocarbons as well as unactivated alkanes. *Nat. Catal.* **2019**, *2*, 1016−1026.
(16) Li, J.; Zhang, Z.; Wu, L.; Zhang, W.; Chen, P.; Lin, Z.; Liu, G. Site-specific allylic C-H bond functionalization with a copper-bound N-centred radical. *Nature* **2019**, *574*, 516−521.
(17) Zuo, Z.; Ahneman, D. T.; Chu, L.; Terrett, J. A.; Doyle, A. G.; MacMillan, D. W. C. Merging Photoredox with Nickel Catalysis: Coupling of α-Carboxyl sp^3-Carbons with Aryl Halides. *Science* **2014**, *345*, 437−440.
(18) Tellis, J. C.; Primer, D. N.; Molander, G. A. Single-Electron Transmetalation in Organoboron Cross-Coupling by Photoredox/Nickel Dual Catalysis. *Science* **2014**, *345*, 433−436.
(19) Twilton, J.; Le, C.; Zhang, P.; Shaw, M. H.; Evans, R. W.; MacMillan, D. W. C. The Merger of Transition Metal and Photocatalysis. *Nat. Rev. Chem.* **2017**, *1*, 0052.
(20) Wang, C.-S.; Dixneuf, P. H.; Soulé, J. F. Photoredox Catalysis for Building C-C Bonds from C(sp^2)-H Bonds. *Chem. Rev.* **2018**, *118*, 7532−7585.
(21) Milligan, J. A.; Phelan, J. P.; Badir, S. O.; Molander, G. A. Alkyl Carbon-Carbon Bond Formation by Nickel/Photoredox Cross-Coupling. *Angew. Chem., Int. Ed.* **2019**, *58*, 6152−6163.
(22) Cheng, W.-M.; Shang, R. Transition Metal-Catalyzed Organic Reactions under Visible Light: Recent Developments and Future Perspectives. *ACS Catal.* **2020**, *10*, 9170−9196.
(23) Zhu, C.; Yue, H.; Jia, J.; Rueping, M. Nickel-Catalyzed C-Heteroatom Cross-Coupling Reactions under Mild Conditions via Facilitated Reductive Elimination. *Angew. Chem., Int. Ed.* **2021**, *60*, 17810−17831.
(24) Cheung, K. P. S.; Sarkar, S.; Gevorgyan, V. Visible Light-Induced Transition Metal Catalysis. *Chem. Rev.* **2022**, *122*, 1543−1625.
(25) Lipp, A.; Badir, S. O.; Molander, G. A. Stereoinduction in Metallaphotoredox Catalysis. *Angew. Chem., Int. Ed.* **2021**, *60*, 1714−1726.
(26) Mondal, S.; Dumur, F.; Gigmes, D.; Sibi, M. P.; Bertrand, M. P.; Nechab, M. Enantioselective Radical Reactions Using Chiral Catalysts. *Chem. Rev.* **2022**, *122*, 5842−5976.
(27) Kariofillis, S. K.; Doyle, A. G. Synthetic and Mechanistic Implications of Chlorine Photoelimination in Nickel/Photoredox C(sp^3)-H Cross-Coupling. *Acc. Chem. Res.* **2021**, *54*, 988−1000.
(28) Chan, A. Y.; Perry, I. B.; Bissonnette, N. B.; Buksh, B. F.; Edwards, G. A.; Frye, L. I.; Garry, O. L.; Lavagnino, M. N.; Li, B. X.; Liang, Y.; Mao, E.; Millet, A.; Oakley, J. V.; Reed, N. L.; Sakai, H. A.; Seath, C. P.; MacMillan, D. W. C. Metallaphotoredox: The Merger of Photoredox and Transition Metal Catalysis. *Chem. Rev.* **2022**, *122*, 1485−1542.
(29) Holmberg-Douglas, N.; Nicewicz, D. A. Photoredox-Catalyzed C-H Functionalization Reactions. *Chem. Rev.* **2022**, *122*, 1925−2016.
(30) Pezzetta, C.; Bonifazi, D.; Davidson, R. W. M. Enantioselective Synthesis of *N*-Benzylic Heterocycles: A Nickel and Photoredox Dual Catalysis Approach. *Org. Lett.* **2019**, *21*, 8957−8961.
(31) Rand, A. W.; Yin, H.; Xu, L.; Giacoboni, J.; Martin-Montero, R.; Romano, C.; Montgomery, J.; Martin, R. Dual Catalytic Platform for Enabling sp^3 α C-H Arylation and Alkylation of Benzamides. *ACS Catal.* **2020**, *10*, 4671−4676.
(32) Shu, X.; Huan, L.; Huang, Q.; Huo, H. Direct Enantioselective C(sp^3)-H Acylation for the Synthesis of α-Amino Ketones. *J. Am. Chem. Soc.* **2020**, *142*, 19058−19064.
(33) Shu, X.; Zhong, D.; Lin, Y.; Qin, X.; Huo, H. Modular Access to Chiral α-(Hetero)aryl Amines via Ni/Photoredox Catalyzed Enantioselective Cross-Coupling. *J. Am. Chem. Soc.* **2022**, *144*, 8797−8806.
(34) Cheng, X.; Lu, H.; Lu, Z. Enantioselective benzylic C-H arylation via photoredox and nickel dual catalysis. *Nat. Commun.* **2019**, *10*, No. 3549.
(35) Cheng, X.; Li, T.; Liu, Y.; Lu, Z. Stereo- and Enantioselective Benzylic C-H Alkenylation via Photoredox/Nickel Dual Catalysis. *ACS Catal.* **2021**, *11*, 11059−11065.
(36) Xu, J.; Li, Z.; Xu, Y.; Shu, X.; Huo, H. Stereodivergent Synthesis of Both *Z*- and *E*-Alkenes by Photoinduced, Ni-Catalyzed Enantioselective C(sp^3)-H Alkenylation. *ACS Catal.* **2021**, *11*, 13567−13574.
(37) Shen, Y.; Gu, Y.; Martin, R. sp^3 C-H Arylation and Alkylation Enabled by the Synergy of Triplet Excited Ketones and Nickel Catalysts. *J. Am. Chem. Soc.* **2018**, *140*, 12200−12209.
(38) Fuse, H.; Kojima, M.; Mitsunuma, H.; Kanai, M. Acceptorless dehydrogenation of hydrocarbons by noble-metal free hybrid catalyst system. *Org. Lett.* **2018**, *20*, 2042−2045.
(39) Kawasaki, T.; Ishida, N.; Murakami, M. Photoinduced Specific Acylation of Phenolic Hydroxy Groups with Aldehydes. *Angew. Chem., Int. Ed.* **2020**, *59*, 18267−18271.
(40) Ritu; Das, S. R.; Tian, Y.; Karl, T.; Jain, N.; Konig, B. Photocatalyzed Dehydrogenation of Aliphatic N-Heterocycles Releasing Dihydrogen. *ACS Catal.* **2022**, *12*, 10326−10332.
(41) Wang, K.; Ding, Z.; Zhou, Z.; Kong, W. Ni-Catalyzed Enantioselective Reductive Diarylation of Activated Alkenes by Domino Cyclization/Cross-Coupling. *J. Am. Chem. Soc.* **2018**, *140*, 12364−12368.
(42) Desrosiers, J.-N.; Wen, J.; Tcyrulnikov, S.; Biswas, S.; Qu, B.; Hie, L.; Kurouski, D.; Wu, L.; Grinberg, N.; Haddad, N.; Busacca, C. A.; Yee, N. K.; Song, J. J.; Garg, N. K.; Zhang, X.; Kozlowski, M. C.; Senanayake, C. H. Enantioselective Nickel-Catalyzed Mizoroki−Heck Cyclizations To Generate Quaternary Stereocenters. *Org. Lett.* **2017**, *19*, 3338−3341.
(43) Huang, X.; Teng, S.; Chi, Y.; Xu, W.; Pu, M.; Wu, Y.; Zhou, J. Enantioselective Intermolecular Heck and Reductive Heck Reactions of Aryl Triflates, Mesylates and Tosylates Catalyzed by Nickel. *Angew. Chem., Int. Ed.* **2021**, *60*, 2828−2832.
(44) Dewanji, A.; Krach, P. E.; Rueping, M. The dual role of benzophenone in visible-light/nickel photoredox-catalyzed C-H

https://doi.org/10.1021/jacs.2c12481
J. Am. Chem. Soc. XXXX, XXX, XXX−XXX

arylations: hydrogen-atom transfer and energy transfer. *Angew. Chem., Int. Ed.* **2019**, *58*, 3566−3570.
(45) Campbell, M. W.; Yuan, M.; Polites, V. C.; Gutierrez, O.; Molander, G. A. Photochemical C-H Activation Enables Nickel-Catalyzed Olefin Dicarbofunctionalization. *J. Am. Chem. Soc.* **2021**, *143*, 3901−3910.
(46) Gu, Y.; Yin, H.; Wakeling, M.; An, J.; Martin, R. Defunctionalization of sp^3 C-Heteroatom and sp^3 C-C Bonds Enabled by Photoexcited Triplet Ketone Catalysts. *ACS Catal.* **2022**, *12*, 1031−1036.
(47) Heitz, D. R.; Tellis, J. C.; Molander, G. A. Photochemical nickel-catalyzed C-H arylation: synthetic scope and mechanistic investigations. *J. Am. Chem. Soc.* **2016**, *138*, 12715−12718.
(48) Shaw, M. H.; Shurtleff, V. W.; Terrett, J. A.; Cuthbertson, J. D.; MacMillan, D. W. C. Native functionality in triple catalytic cross-coupling: sp^3 C-H bonds as latent nucleophiles. *Science* **2016**, *352*, 1304−1308.
(49) Shields, B. J.; Doyle, A. G. Direct C(sp^3)-H cross coupling enabled by catalytic generation of chlorine radicals. *J. Am. Chem. Soc.* **2016**, *138*, 12719−12722.
(50) Nielsen, M. K.; Shields, B. J.; Liu, J.; Williams, M. J.; Zacuto, M. J.; Doyle, A. G. Mild, redox-neutral formylation of aryl chlorides through the photocatalytic generation of chlorine radicals. *Angew. Chem., Int. Ed.* **2017**, *56*, 7191−7194.
(51) Deng, H.-P.; Fan, X.-Z.; Chen, Z.-H.; Xu, Q.-H.; Wu, J. Photoinduced nickelcatalyzed chemo- and regioselective hydroalkylation of internal alkynes with ether and amide α-hetero C(sp^3)-H bonds. *J. Am. Chem. Soc.* **2017**, *139*, 13579−13584.
(52) Le, C.; Liang, Y.; Evans, R. W.; Li, X.; MacMillan, D. W. C. Selective sp^3 C-H alkylation via polarity-match-based cross-coupling. *Nature* **2017**, *547*, 79−83.
(53) Perry, I. B.; Brewer, T. F.; Sarver, P. J.; Schultz, D. M.; DiRocco, D. A.; MacMillan, D. A. C. Direct arylation of strong aliphatic C-H bonds. *Nature* **2018**, *560*, 70−75.
(54) Hwang, S. J.; Powers, D. C.; Maher, A. G.; Anderson, B. L.; Hadt, R. G.; Zheng, S.-L.; Chen, Y.-S.; Nocera, D. G. Trap-Free Halogen Photoelimination from Mononuclear Ni(III) Complexes. *J. Am. Chem. Soc.* **2015**, *137*, 6472−6475.
(55) Deng, H.-P.; Fan, X.; Chen, Z.; Xu, Q.; Wu, J. Photoinduced Nickel-Catalyzed Chemo- and Regioselective Hydroalkylation of Internal Alkynes with Ether and Amide α-Hetero C(sp^3)-H Bonds. *J. Am. Chem. Soc.* **2017**, *139*, 13579−13584.
(56) Treacy, S. M.; Rovis, T. Copper Catalyzed C(sp^3)-H Bond Alkylation via Photoinduced Ligand-to-Metal Charge Transfer. *J. Am. Chem. Soc.* **2021**, *143*, 2729−2735.
(57) Gonzalez, M. I.; Gygi, D.; Qin, Y.; Zhu, Q.; Johnson, E. J.; Chen, Y. S.; Nocera, D. G. Taming the Chlorine Radical: Enforcing Steric Control over Chlorine-Radical-Mediated C-H Activation. *J. Am. Chem. Soc.* **2022**, *144*, 1464−1472.
(58) Bhattacharya, S. K.; Cameron, K. O. K.; Dowling, M. S.; Fernando, D. P.; Ebner, D. C.; Filipski, K. J.; Kung, D. W.; Lee, E. C. Y.; Smith, A. C.; Tu, M. M. Preparation of Indole and Indazole Compounds That Activate AMPK. WO20141407042018.
(59) (a) Rej, R. K.; Tapas, D.; Suman, H.; Samik, N. Chemo-enzymatic asymmetric synthesis of fluoxetine, atomoxetine, nisoxetine, and duloxetine. *Tetrahedron: Asymmetry* **2013**, *24*, 913−918. (b) Deng, C.-Q.; Deng, J. Ni-Catalyzed Asymmetric Hydrogenation of Aromatic Ketoacids for the Synthesis of Chiral Lactones. *Org. Lett.* **2022**, *24*, 2494−2498.
(60) Hilborn, J. W.; Lu, Z.-H.; Jurgens, A. R.; Fang, Q. K.; Byers, P.; Wald, S. A.; Senanayake, C. H. A practical asymmetric synthesis of (*R*)-fluoxetine and its major metabolite (*R*)-norfluoxetine. *Tetrahedron Lett.* **2001**, *42*, 8919−8921.
(61) Seebach, D.; Zimmermann, J.; Gysel, U.; Ziegler, R.; Ha, T. Totally Stereoselective Additions to 2,6-Disubstituted l,3-Dioxin-4-ones (Chiral Acetoacetic Acid Derivatives). Synthetic and Mechanistic Aspects of Remote Stereoselectivity. *J. Am. Chem. Soc.* **1988**, *110*, 4763−4772.
(62) Koyama, K.; Naruto, S.; Kaneko, T. Preparation of Piperidines as Acetylcholine Esterase Inhibitors and Selective Serotonin Reuptake Inhibitors. JP2000219678 A2000.
(63) Matsuda, H.; Nakamura, S.; Iwami, J.; Li, X.; Pongpiriyadacha, Y.; Nakai, M.; Kubo, M.; Fukuyama, Y.; Yoshikawa, M. Invasion Inhibitors of Human Fibrosarcoma HT 1080 Cells from the Rhizomes of *Zingiber cassumunar*: Structures of Phenylbutanoids, Cassumunols. *Chem. Pharm. Bull.* **2011**, *59*, 365−370.
(64) Kasai, S.; Kamaura, M.; Cho, N. Preparation of Heterocyclic Compounds As Retinol Binding Protein 4 (RBP4) Lowering Agents. WO20091452862009.
(65) Skubi, K. L.; Blum, T. R.; Yoon, T. P. Dual Catalysis Strategies in Photochemical Synthesis. *Chem. Rev.* **2016**, *116*, 10035−10074.
(66) Maity, B.; Scott, T. R.; Stroscio, G. D.; Gagliardi, L.; Cavallo, L. The Role of Excited States of $LNi^{II/III}$(Aryl)(Halide) Complexes in Ni-Halide Bond Homolysis in the Arylation of Csp^3-H Bonds. *ACS Catal.* **2022**, *12*, 13215−13224.
(67) Falivene, L.; Cao, Z.; Petta, A.; Serra, L.; Poater, A.; Oliva, R.; Scarano, V.; Cavallo, L. Towards the online computer-aided design of catalytic pockets. *Nat. Chem.* **2019**, *11*, 872−879.
(68) Maity, B.; Zhu, C.; Yue, H.; Huang, L.; Harb, M.; Minenkov, Y.; Rueping, M.; Cavallo, L. Mechanistic Insight into the Photoredox-Nickel-HAT Triple Catalyzed Arylation and Alkylation of α-Amino Csp^3-H Bonds. *J. Am. Chem. Soc.* **2020**, *142*, 16942−16952.
(69) Wang, S.; Ma, P.; Shaik, S.; Che, H. Valence-Inverted States of Nickel(II) Complexes Perform Facile C-H Bond Activation. *J. Am. Chem. Soc.* **2022**, *144*, 14607−14613.
(70) Bour, J. R.; Camasso, N. M.; Sanford, M. S. Oxidation of Ni(II) to Ni(IV) with Aryl Electrophiles Enables Ni-Mediated Aryl-CF_3 Coupling. *J. Am. Chem. Soc.* **2015**, *137*, 8034−8037.
(71) Watson, M. B.; Rath, N. P.; Mirica, L. M. Oxidative C-C Bond Formation Reactivity of Organometallic Ni(II), Ni(III), and Ni(IV) Complexes. *J. Am. Chem. Soc.* **2017**, *139*, 35−38.

https://doi.org/10.1021/jacs.2c12481
J. Am. Chem. Soc. XXXX, XXX, XXX−XXX